Nanoscale

ROYAL SOCIETY OF CHEMISTRY

COMMUNICATION

View Article Online
View Journal | View Issue

Open Access Article. Published on 05 May 2025. Downloaded on 1/21/2026 8:44:58 AM.
This article is licensed under a Creative Commons Attribution-NonCommercial 3.0 Unported Licence.

Check for updates

Cite this: *Nanoscale*, 2025, **17**, 13207

Received 21st March 2025,
Accepted 3rd May 2025

DOI: 10.1039/d5nr01176k

rsc.li/nanoscale

Azido-enabled thermal history analysis on a metal–oxide surface†

Satoki Yamaguchi,[a] Tomohiro Iwai, *[a] Hiromichi V. Miyagishi,[a] Hiroshi Masai,[a] Takuro Hosomi,[b] Takeshi Yanagida,[b] Ken Uchida[c] and Jun Terao *[a]

A novel strategy for localized thermal history analysis using organic azides immobilized on ZnO nanowire arrays is presented. The pyrolysis of the surface azido groups followed by the introduction of molecular probes to the residual azido groups *via* the Huisgen cycloaddition enables microscale temperature distribution measurement using scanning electron microscopy–energy-dispersive X-ray spectrometry analysis.

With the miniaturization of inorganic devices for sensors and catalysts, localized thermal measurements of solid materials have become increasingly important to ensure their stable operation and maximum performance.[1–5] Recently, organic molecules have been used as probes for the thermal measurements of inorganic materials owing to their structural diversity, enabling accurate and versatile temperature measurements.[6–9] Among these approaches, the irreversible transformation of temperature-sensitive organic molecules has been leveraged to record thermal history, providing insights into the temperature variations experienced during thermal events.[10–12] This recording strategy can also be applied to operating devices, where real-time temperature measurement may be challenging. However, the use of organic molecules for analyzing the thermal history of solid materials remains limited owing to requirements such as clean irreversible changes for the recording and space-resolved analysis for the readout. Recently, we measured the nanometer-scale temperature distribution in Joule-heated gold nanosheet gas sensors through the thermal desorption of fluorinated alkanethiol self-assembled monolayers (SAMs), an irreversible process in which the molecular structure remained nearly unchanged.[13]

Herein, we introduce a novel strategy for localized thermal history analysis using the thermally irreversible transformation of organic molecules immobilized on metal oxide surfaces. To this end, we leverage organic azides, which exhibit unique reactivity toward pyrolysis[14–16] and the Huisgen cycloaddition.[17–19] The proposed approach can be summarized as follows (Fig. 1): the surface azido groups immobilized on metal oxides undergo irreversible thermal decomposition and loss of molecular nitrogen, allowing the heat exposure to be recorded. Subsequently, molecular probes for space-resolved spectroscopic readout are introduced to the residual azido groups *via* the Huisgen cycloaddition. The resulting framework allows the recorded temperature to be measured with high spatial resolution. The use of SAMs to introduce organic azides onto metal oxide surfaces ensures a uniform reaction field through ordered molecular orientation.[20–28] The feasibility of the proposed approach is demonstrated through micrometer-scale thermal history analysis based on localized Joule heating for azide pyrolysis recording and scanning electron microscopy–energy-dispersive X-ray spectrometry (SEM-EDS) analysis for non-destructive and space-resolved readout.[29]

We first investigated the validity of the azido-enabled thermal history analysis under macro-heating conditions.

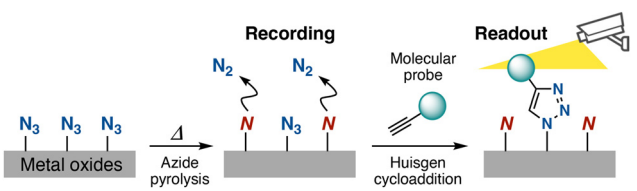

Fig. 1 Conceptual view of the proposed azido-enabled thermal history analysis system. "N", shown in italicized, red font, indicates the chemical species in which the nitrogen molecule has been eliminated from the surface azido group, but the resulting structure remains to be identified.

[a]*Department of Basic Science, Graduate School of Arts and Sciences, The University of Tokyo, 3-8-1, Komaba, Meguro-ku, Tokyo, 153-8902, Japan.*
E-mail: ciwai@g.ecc.u-tokyo.ac.jp, cterao@g.ecc.u-tokyo.ac.jp
[b]*Department of Applied Chemistry, Graduate School of Engineering, The University of Tokyo, Bunkyo-ku, Tokyo 113-8656, Japan*
[c]*Department of Materials Engineering, Graduate School of Engineering, The University of Tokyo, Bunkyo-ku, Tokyo 113-8656, Japan*

† Electronic supplementary information (ESI) available: Experimental procedures and compound characterization. See DOI: https://doi.org/10.1039/d5nr01176k

Open Access Article. Published on 05 May 2025. Downloaded on 1/21/2026 8:44:58 AM.
This article is licensed under a Creative Commons Attribution-NonCommercial 3.0 Unported Licence.

Azido-terminated SAMs were fabricated on ZnO nanowire arrays (ZnO NWs) with uniform size and large surface areas to enhance detection intensity in spectroscopic analyses. This was achieved using our previous procedure with a slight modification.[30] Specifically, ZnO NWs grown on a silicon substrate and modified with (12-azidododecyl)phosphonic acid (**1/ZnO-NW**) were uniformly heated at 220 °C on a hotplate, and pyrolysis of the azido group was monitored through Fourier-transform infrared (FT-IR) spectroscopy (Fig. 2a). As shown in Fig. 2b, the peak at 2103 cm^{-1}, corresponding to the azido groups, decreased following first-order kinetics with a reaction rate constant (k_{220}) of 0.061 min^{-1}.[31] When the same experiments were conducted at 200 °C and 235 °C (Fig. 2c), the reaction rate constants k_{200} and k_{235} were 0.014 min^{-1} and 0.135 min^{-1}, respectively. An Arrhenius plot constructed from these reaction rate constants showed that the pyrolysis activation energy of the surface azido group was 147 kJ mol^{-1} (Fig. 2d). This value is comparable to reported organic azides,[32] indicating that the immobilization did not affect the azide pyrolysis.

To enhance the spatial resolution in tracing the pyrolysis of surface azido groups compared with typical FT-IR measurements, elemental mapping was performed using SEM-EDS, following the introduction of an EDS-active molecular probe to the residual azido group *via* the Huisgen cycloaddition. Specifically, an ethynyl-tethered pentachlorophenol derivative (**5Cl**) was adopted as the EDS probe for Cl owing to its independent and strong peak signal (Fig. S7†). In this process, **1/**

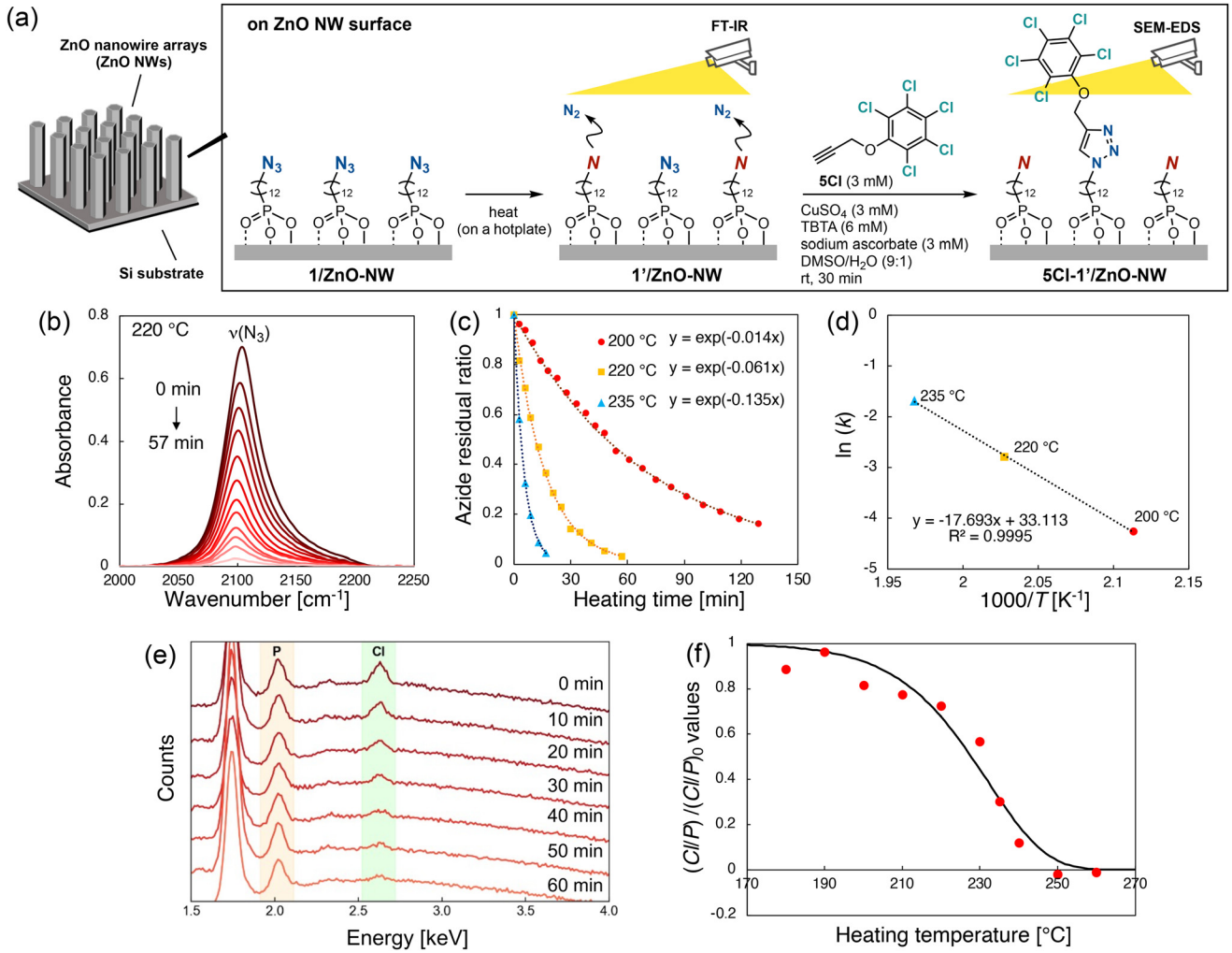

Fig. 2 Scheme and the spectroscopic trace of azide pyrolysis followed by the Huisgen cycloaddition using **1/ZnO-NW**: (a) reaction scheme of azide pyrolysis of **1/ZnO-NW** and the subsequent Huisgen cycloaddition between **1'/ZnO-NW** and **5Cl** (TBTA, tris[(1-benzyl-1*H*-1,2,3-triazol-4-yl)methyl] amine; DMSO, dimethyl sulfoxide). (b) FT-IR spectral variation in the azido region on **1/ZnO-NW** at 220 °C (heating time: 0, 3, 9, 13, 17, 21, 25, 30, 35, 41, 48, and 57 min). (c) Time-dependent conversion rate of the surface azido group, normalized to the initial amount of **1/ZnO-NW** (red circles for 200 °C, yellow squares for 220 °C, and blue triangles for 235 °C). (d) Arrhenius plot constructed from the rate constants of surface azide pyrolysis. (e) SEM-EDS spectral variation in **5Cl-1'/ZnO-NW** depending on the heating time (220 °C; 0, 10, 20, 30, 40, 50, and 60 min). (f) Calibration curve obtained by fitting the measured $(Cl/P)/(Cl/P)_0$ values of **5Cl-1'/ZnO-NW**, based on SEM-EDS analysis (heating temperature: 180, 190, 200, 210, 220, 230, 235, 240, 250, and 260 °C for 10 min).

Open Access Article. Published on 05 May 2025. Downloaded on 1/21/2026 8:44:58 AM.
This article is licensed under a Creative Commons Attribution-NonCommercial 3.0 Unported Licence.

ZnO-NW were heated at 220 °C on a hotplate, and the resulting substrate (**1′/ZnO-NW**) was immersed in a dimethyl sulfoxide (DMSO)/H_2O solution of **5Cl** in the presence of $CuSO_4$, tris[(1-benzyl-1*H*-1,2,3-triazol-4-yl)methyl]amine (TBTA), and sodium ascorbate for 30 min to obtain **5Cl-1′/ZnO-NW** (Fig. 2a). Fig. 2e shows the SEM-EDS spectra of **5Cl-1′/ZnO-NW** in the 3 μm × 4 μm range for different heating durations (0, 10, 20, 30, 40, 50, and 60 min). The Cl signal at 2.6 keV decreased with increasing heating time, whereas that of P, derived from the phosphonic acid anchor at 2.0 keV, remained constant. This suggests that the SAM molecules did not desorb from the ZnO NW surface during the substrate heating followed by the Huisgen cycloaddition. Incomplete azido conversion was observed during the Huisgen cycloaddition owing to the steric hindrance between adjacent azido groups (Fig. S8†).[30] However, this did not directly affect the thermal history analysis.

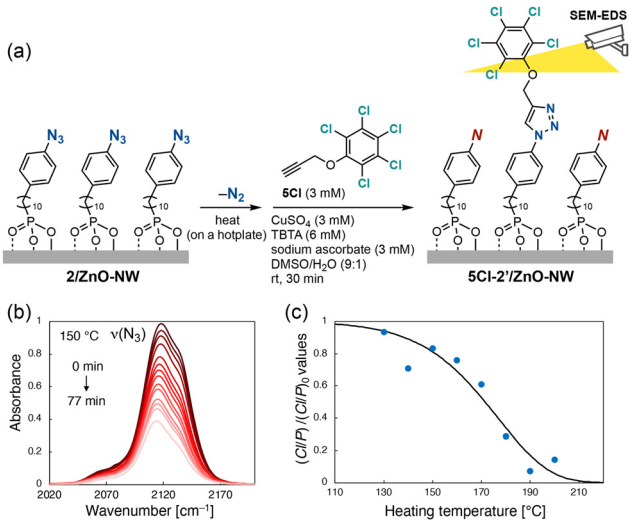

Fig. 3 Scheme and the spectroscopic trace of azide pyrolysis followed by the Huisgen cycloaddition using **2/ZnO-NW**: (a) reaction scheme of azide pyrolysis of **2/ZnO-NW** and the subsequent Huisgen cycloaddition with **5Cl**. (b) FT-IR spectral variation in the azido region on **2/ZnO-NW** at 150 °C (heating time: 0, 3, 6, 10, 14, 18, 23, 28, 33, 39, 45, 51, 57, 63, 70, and 77 min). (c) Calibration curve obtained by fitting the measured $(Cl/P)/(Cl/P)_0$ values of **5Cl-2′/ZnO-NW**, based on SEM-EDS analysis (heating temperature: 130, 140, 150, 160, 170, 180, 190, and 200 °C for 10 min).

To determine the heating temperature from SEM-EDS measurements, the Cl signal intensity relative to the P signal intensity (denoted as Cl/P) after heating at various temperatures was plotted. Specifically, **1/ZnO-NW** samples were uniformly heated on a hotplate at 180–260 °C for 10 min, and the EDS-probe **5Cl** was then introduced to the residual azido group *via* the Huisgen cycloaddition. As shown in Fig. 2f, the normalized signal values relative to the initial level at each temperature, $(Cl/P)/(Cl/P)_0$, decreased with increasing temperature, corresponding to the azide pyrolysis ratio determined by FT-IR analysis (Fig. 2b). A temperature calibration curve based on SEM-EDS results was obtained by fitting the $(Cl/P)/(Cl/P)_0$ values as follows (eqn (1)):

$$\frac{(Cl/P)}{(Cl/P)_0} = \exp\left\{-A\exp\left(-\frac{E_a}{RT}\right)\times t\right\} \quad (1)$$

where E_a is the activation energy, R is the universal gas constant, T is the temperature, A is the pre-exponential factor, and t is the heating time (see Fig. S12 in the ESI† for details of the preparation of the calibration curve and its uncertainty).

To assess the thermal history at lower temperatures, the thermal recording unit was changed from an alkyl azide to an aryl azide, which exhibits higher susceptibility to pyrolysis.[15] Specifically, (10-(4-azidophenyl)decyl)phosphonic acid (**2**) was immobilized on ZnO NWs grown on a silicon substrate using the same procedure as that for **1**. The resulting **2/ZnO-NW** samples underwent pyrolysis at approximately 150 °C, as observed by FT-IR monitoring at 2120 cm^{-1} (Fig. 3a and b). The Huisgen cycloaddition of the residual azido groups with **5Cl** followed by SEM-EDS analysis yielded a temperature calibration curve based on eqn (1) (Fig. 3c, S14†). The trend was consistent with the azide pyrolysis rate based on the FT-IR analysis. However, the deviation was larger compared with the trends for **1/ZnO-NW**. This difference is attributable to the

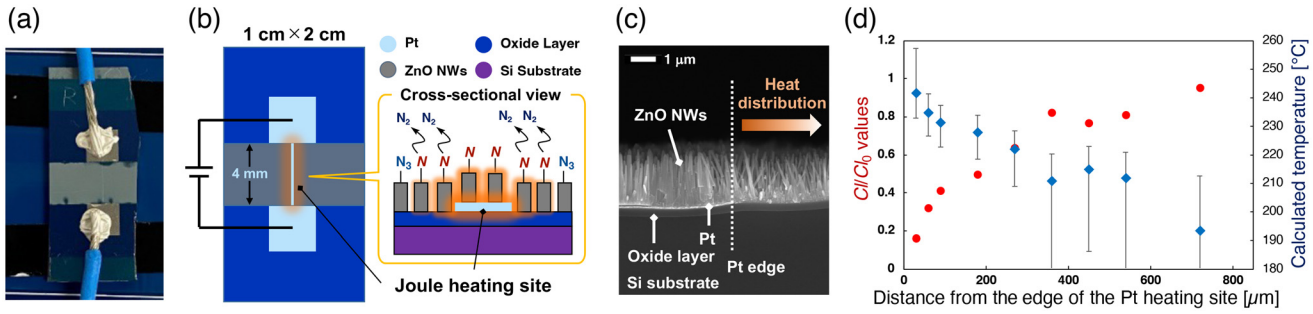

Fig. 4 Thermal history analysis in an actual device equipped with a localized Joule heating system: (a) photograph and (b) schematic of the heating device, **1/ZnO-NW/Pt**. The Pt heating site has dimensions of 4 mm (length) × 10 μm (width) × 200 nm (depth). Joule heating was applied at 80 V for 10 min. (c) Cross-sectional SEM image of the heating device before SAM preparation with **1**. Heat distribution was measured from the edge of the Pt heating site. (d) The Cl signal intensity relative to the initial value in EDS (left) or calculated temperature (right) plotted as a function of distance from the edge of the Pt heating site in **5Cl-1′/ZnO-NW/Pt** (distance: 30, 60, 90, 180, 270, 360, 450, 540, and 720 μm).

Open Access Article. Published on 05 May 2025. Downloaded on 1/21/2026 8:44:58 AM. This article is licensed under a Creative Commons Attribution-NonCommercial 3.0 Unported Licence.

aggregation of the aryl azide group on the ZnO surface owing to π–π interactions, which hinders the Huisgen cycloaddition owing to steric effects (see Fig. S16 and S17 in the ESI† for details of the surface Huisgen cycloaddition with **1**/**ZnO-NW** or **2**/**ZnO-NW**).[33] Although the aryl groups in azido-functionalized SAMs may lead to deviations from the ideal reaction rate in azide pyrolysis, structural variations in the azido molecules can enable thermal history analysis in a specific temperature range.

To demonstrate the utility of the present azido-enabled thermal history analysis system, we prepared heat distribution maps for an actual device equipped with a localized Joule heating system. The heating device, **1**/**ZnO-NW**/**Pt**, was fabricated on a silicon dioxide layer over a silicon substrate using laser lithography, followed by Pt sputtering, ZnO NW growth, and the introduction of azido-functionalized SAMs using **1** (Fig. 4a–c). After Joule heating at the Pt heating site (4 mm (length) × 10 μm (width) × 200 nm (depth)) at 80 V for 10 min for azide pyrolysis, the EDS-probe **5Cl** was introduced into the residual azido groups to form **5Cl-1′**/**ZnO-NW**/**Pt**. As shown in Fig. 4d, sequential SEM-EDS analysis of **5Cl-1′**/**ZnO-NW**/**Pt** in the 3 μm × 4 μm range allowed the calculation of the heat distribution from the edge of the Pt heating site across several hundred micrometers, using the calibration curve shown in Fig. 2f (see the ESI† for details of the calibration uncertainty).

Conclusions

In summary, we developed a novel method for localized thermal history analysis using azido-terminated SAMs immobilized on ZnO NWs. Pyrolysis of the surface azido groups, followed by the introduction of the EDS-active molecular probe **5Cl** to the residual azido groups through the Huisgen cycloaddition, enabled heat distribution mapping with a microscale resolution *via* SEM-EDS analysis. Using alkyl azide **1** and aryl azide **2**, which have different thermal decomposition temperatures, the thermal history could be measured over a wide temperature range. The utility of this framework was demonstrated by recording the thermal history of microscale temperature differences in a localized Joule-heated device. Future work will be aimed at expanding the applicability of the proposed method to sensors and catalysts in operation, where real-time thermal measurement is difficult.

Author contributions

T. I. and J. T. conceived and supervised the idea. S. Y. performed all experiments. All authors discussed the results and wrote the manuscript.

Data availability

The data supporting this article have been included as part of the ESI.†

Conflicts of interest

There are no conflicts to declare.

Acknowledgements

This research was partially supported by JSPS KAKENHI Grant Numbers JP22K19022 (T. I.), JP25H01647 (T. I.), JP25K01761 (T. I.), JP22H02060 (J. T.), JP24KK0111 (T. I., J. T.), and JP25H00892 (J. T.), JST CERST Grant Number JPMJCR19I2 (J. T., T. Y., and K. U.), JST SPRING Grant Number JPMJSP2108 (S. Y.), the Canon Foundation (J. T.), the Toshiaki Ogasawara Memorial Foundation (T. I., J. T.), the Iketani Science and Technology Foundation (J. T.), and the Uehara Memorial Foundation (J. T.). We thank Prof. Sayaka Uchida and Prof. Naoki Ogiwara (Graduate School of Arts and Sciences, The University of Tokyo) for thermogravimetric analysis. We also thank Ms Karin Nishimura (Graduate School of Engineering, Kyoto University) for the high-resolution mass spectral measurements of **2**.

References

1 Y. Yue and X. Wang, *Nano Rev.*, 2012, **3**, 11586.
2 C. D. S. Brites, P. P. Lima, N. J. O. Silva, A. Millán, V. S. Amaral, F. Palacio and L. D. Carlos, *Nanoscale*, 2012, **4**, 4799–4829.
3 M. Quintanilla and L. M. Liz-Marzán, *Nano Today*, 2018, **19**, 126–145.
4 T. Hartman, R. G. Geitenbeek, G. T. Whiting and B. M. Weckhuysen, *Nat. Catal.*, 2019, **2**, 986–996.
5 M. Filez, V. De Coster, H. Poelman, V. Briois, A. Beauvois, J. Dendooven, M. B. J. Roeffaers, V. Galvita and C. Detavernier, *Nat. Catal.*, 2025, **8**, 187–195.
6 M. M. Ogle, A. D. S. McWilliams, B. Jiang and A. A. Martí, *ChemPhotoChem*, 2020, **4**, 255–270.
7 Y. Sun, M. Fu, M. Bian and Q. Zhu, *Biotechnol. Bioeng.*, 2023, **120**, 7–21.
8 M. Rodrigues, R. Piñol, G. Antorrena, C. D. S. Brites, N. J. O. Silva, J. L. Murillo, R. Cases, I. Díez, F. Palacio, N. Torras, J. A. Plaza, L. Pérez-García, L. D. Carlos and A. Millán, *Adv. Funct. Mater.*, 2016, **26**, 200–209.
9 S. Hu, B.-J. Liu, J.-M. Feng, C. Zong, K.-Q. Lin, X. Wang, D.-Y. Wu and B. Ren, *J. Am. Chem. Soc.*, 2018, **140**, 13680–13686.
10 L. Yang, E. Zhao, G. Wang, X. Yu and X. Gu, *ACS Appl. Mater. Interfaces*, 2024, **16**, 25294–25303.
11 Y. Yang, Y. Wu, D. Mei and Y. Qu, *Chem. Eng. J.*, 2019, **358**, 606–613.
12 Y. Tominaga, S. Kanemitsu, S. Yamamoto, T. Kimura, Y. Nishida, K. Morita and T. Maruyama, *Colloids Surf., A*, 2023, **656**, 130416.
13 T. Kato, T. Tanaka, H. Miyagishi, J. Terao and K. Uchida, *2023 7th IEEE Electron Devices Technology and Manufacturing Conference (EDTM) 2023*. DOI: 10.1109/EDTM55494.2023.10103112.

 This journal is © The Royal Society of Chemistry 2025

Open Access Article. Published on 05 May 2025. Downloaded on 1/21/2026 8:44:58 AM.
This article is licensed under a Creative Commons Attribution-NonCommercial 3.0 Unported Licence.

14 J. H. Boyer and F. C. Canter, *Chem. Rev.*, 1954, **54**, 1–57.
15 G. L'abbe, *Chem. Rev.*, 1969, **69**, 345–363.
16 H. Bock and R. Dammel, *Angew. Chem., Int. Ed. Engl.*, 1987, **26**, 504–526.
17 M. Meldal and C. W. Tornøe, *Chem. Rev.*, 2008, **108**, 2952–3015.
18 L. Liang and D. Astruc, *Coord. Chem. Rev.*, 2011, **255**, 2933–2945.
19 M. Breugst and H.-U. Reissig, *Angew. Chem., Int. Ed.*, 2020, **59**, 12293–12307.
20 S. Onclin, B. J. Ravoo and D. N. Reinhoudt, *Angew. Chem., Int. Ed.*, 2005, **44**, 6282–6304.
21 S. P. Pujari, L. Scheres, A. T. M. Marcelis and H. Zuilhof, *Angew. Chem., Int. Ed.*, 2014, **53**, 6322–6356.
22 M. Li, M. Liu, F. Qi, F. R. Lin and A. K.-Y. Jen, *Chem. Rev.*, 2024, **124**, 2138–2204.
23 C. Nicosia and J. Huskens, *Mater. Horiz.*, 2014, **1**, 32–45.
24 G. M. Ziarani, Z. Hassanzadeh, P. Gholamzadeh, S. Asadi and A. Badiei, *RSC Adv.*, 2016, **6**, 21979–22006.
25 P. Yáñez-Sedeño, A. González-Cortés, S. Campuzano and J. M. Pingarrón, *Sensors*, 2019, **19**, 2379.
26 M. A. White, J. A. Johnson, J. T. Koberstein and N. J. Turro, *J. Am. Chem. Soc.*, 2006, **128**, 11356–11357.
27 J. Nakazawa, B. J. Smith and T. D. P. Stack, *J. Am. Chem. Soc.*, 2012, **134**, 2750–2759.
28 J. Lee, S. Z. Hassan, S. Lee, H. R. Sim and D. S. Chung, *Nat. Commun.*, 2022, **13**, 7021.
29 D. E. Newbury and N. W. M. Ritchie, *Scanning*, 2013, **35**, 141–168.
30 R. Yamaguchi, T. Hosomi, M. Otani, K. Nagashima, T. Takahashi, G. Zhang, M. Kanai, H. Masai, J. Terao and T. Yanagida, *Langmuir*, 2021, **37**, 5172–5179.
31 A related report on the degradation of surface-bound azido groups with zero-order reaction kinetics: S. S. T. Vandenbroucke, M. Nisula, R. Petit, R. Vos, K. Jans, P. M. Vereecken, J. Dendooven and C. Detavernier, *Langmuir*, 2021, **37**, 12608–12615.
32 C. Wentrup, *Aust. J. Chem.*, 2013, **66**, 852–863.
33 Q.-C. Jiang, T. Iwai, M. Jo, T. Hosomi, T. Yanagida, K. Uchida, K. Hashimoto, T. Nakazono, Y. Yamada, A. Kobayashi, S. Takizawa, H. Masai and J. Terao, *Small*, 2024, **20**, 2403717.